Casey, J, & Threlfall, D. R. (1978) *FEBS Lett. 85*, 249.
Cherest, H., Surdin-Kerjan, Y., & de Robichon-Szulmajster, H. (1971) *J. Bacteriol. 106*, 758.
Cox, G. B., Young, I. G., McCann, C. M., & Gibson, F. (1969) *J. Bacteriol. 99*, 450.
Daves, G. D., Moore, H. W., Schwab, D. E., Olsen, R. K., Wilczynsk, J. J., & Folkers, K. (1967) *J. Org. Chem. 32*, 1414.
Friis, P., Daves, G. D., & Folkers, K. (1966) *J. Am. Chem. Soc. 88*, 4754.
Gibson, F. (1973) *Biochem. Soc. Trans. 1*, 317.
Goewert, R. R., Sippel, C. J., & Olson, R. E. (1977) *Biochem. Biophys. Res. Commun. 77*, 599.
Goewert, R. R., Sippel, C. J., Grimm, M. F., & Olson, R. E. (1978) *FEBS Lett. 87*, 219.
Gordon, P. A., & Stewart, P. R. (1969) *Biochim. Biophys. Acta 177*, 358.
Guldberg, H. C., & Marsden, C. A. (1975) *Pharmacol. Rev. 27*, 135.
Ho, J., Nilsson, J. L. Y., Skelton, F. S., & Folkers, K. I. (1973) *J. Org. Chem. 38*, 1059.
Houser, R. M., & Olson, R. E. (1974) *Life Sci. 14*, 1211.
Houser, R. M., & Olson, R. E. (1977) *J. Biol. Chem. 252*, 4017.
Imamota, S., & Sehoh, H. (1967) *Tetrahedron 13*, 1237.
Morton, R. A. (1965) *Biochemistry of Quinones*, Academic Press, New York.
Muraca, R. F., Daves, G. D., & Folkers, K. (1967) *J. Am. Chem. Soc. 89*, 1505.
Nambudiri, A. M. D., Brockman, D., Alan, S. S., & Rudney, H. (1977) *Biochem. Biophys. Res. Commun. 76*, 282.
Nilsson, G., Farley, T. M., & Folkers, K. (1968) *Anal. Biochem. 23*, 422.
Nowicki, H. G., Dialameh, G. H., & Olson, R. E. (1972) *Biochemistry 11*, 896.
Nyns, E. J., Chiang, N., & Wiaux, A. L. (1968) *Mikrobiol. Zh. (Kiev) 34*, 197.
Olson, R. E. (1966) *Vitam. Horm. (N.Y.) 24*, 551.
Olson, R. E., Bentley, R., Aiyar, A. S., Dialameh, G. H., Gold, P. H., Ramsey, V. G., & Springer, C. M. (1963) *J. Biol. Chem. 238*, PC3146.
Rudney, H., & Parson, W. (1963) *J. Biol. Chem. 238*, P-C3137.
Sherman, F., Stewart, J. W., Parker, J. H., Inhaber, E., Shipman, N. A., Putterman, G. J., Gardisky, R. L., & Margoliash, E. (1968) *J. Biol. Chem. 243*, 5446.
Trumpower, B. L., Aiyar, A. S., Opliger, C. L., & Olson, R. E. (1972) *J. Biol. Chem. 247*, 2499.
Trumpower, B. L., Houser, R. M., & Olson, R. E. (1974) *J. Biol. Chem. 249*, 3041.
Tzagoloff, A., Akai, A., & Needleman, R. B. (1975) *J. Biol. Chem. 250*, 8228.
Whistance, G. R., & Threlfall, D. R. (1967) *Biochem. Biophys. Res. Commun. 28*, 295.
Whistance, G. R., Dillion, J. F., & Threlfall, D. R. (1969) *Biochem. J. 111*, 461.
Whistance, G. R., Brann, B. S., & Threlfall, D. R. (1970) *Biochem. J. 112*, 119.

# Solid-State Carbon-13 Nuclear Magnetic Resonance of the Lecithin Gel to Liquid-Crystalline Phase Transition†

R. J. Wittebort, C. F. Schmidt, and R. G. Griffin*

ABSTRACT: The temperature dependence of the $^{13}C$ NMR spectra of dipalmitoylphosphatidylcholine (DPPC) which has been $^{13}C$ labeled at the carbonyl position of the *sn*-2 chain, 2-[1-$^{13}C$]DPPC, is reported. In the $L_{\beta'}$ phase an axially symmetric spectrum of 112-ppm breadth is observed, and this transforms to an isotropic-like line ($\langle\Delta\sigma\rangle \sim 7$ ppm) in the $L_\alpha$ phase. In the intermediate $P_\beta$ phase a temperature-dependent superposition of these spectra is observed, which suggests that this phase exhibits microscopic structural and dynamical properties of both the $L_{\beta'}$ and $L_\alpha$ phases. An analysis of the spectral line shapes leads to the conclusion that the appearance of the isotropic-like line in the $P_{\beta'}$ phase is primarily due to a conformational change at the *sn*-2 carbonyl which is complete at the main transition. Increased rates of axial diffusion in the $P_{\beta'}$ phase may contribute to the narrowing.

Phase equilibria in the binary lecithin–water system have been the subject of a number of investigations using a variety of structural, spectroscopic, and thermodynamic methods. For aqueous dispersions of dimyristoyl- and dipalmitoylphosphatidylcholine (DMPC and DPPC, respectively), calorimetric measurements identify two endothermic transitions, a broad, low enthalpy pretransition [$T_c'$ = 35.3 °C (DPPC)] and a sharp, high enthalpy main transition [$T_c$ = 41.3 °C (DPPC)] (Chapman et al., 1967). With respect to these different lipid phases, X-ray scattering patterns obtained from unoriented samples have identified the lattice types and dimensions and the general low resolution features of the acyl chain conformations (Tardieu et al., 1973; Janiak et al., 1976, 1979). At temperatures below the pretransition, the lipid molecules are arranged in a one-dimensional, lamellar $L_{\beta'}$ phase in which the acyl chains are predominantly extended (all-trans conformation) and are assumed to be tilted at 30° with respect to the bilayer normal to accommodate the bilayer thickness of 47 Å. For dispersions in excess water, as studied

† From the Francis Bitter National Magnet Laboratory, Massachusetts Institute of Technology, Cambridge, Massachusetts 02139 (R.J.W. and R.G.G.), and the Department of Biochemistry, School of Medicine, University of Virginia 22908 (C.F.S.). *Received December 29, 1980.* This research was supported by National Institutes of Health Grants GM-25505, GM-23289, GM-14628, and RR-00995 and by National Science Foundation Contract C-670 to the Francis Bitter National Magnet Laboratory. R.J.W. is the recipient of a U.S. Public Health Service Postdoctoral Fellowship (GM-07215).

0006-2960/81/0420-4223$01.25/0 

here, there is complete disorder in the plane of the membrane, requiring that the direction of the tilt in the plane of the membrane is also disordered. The acyl chain tilt has been confirmed by X-ray scattering studies on macroscopically oriented samples (Stamatoff et al., 1979). At temperature values between $T_c'$ and $T_c$, a two-dimensional $P_{\beta'}$ or ripple phase is found in which the lamellae of 48-Å thickness undergo periodic undulations of 140-Å length. Also it is postulated that in this phase the acyl chains maintain the tilt angle and the fully extended trans conformation. Recently the ripple structure has been observed by freeze–fracture electron microscopy of phosphatidylcholine dispersions quenched at temperature values between $T_c'$ and $T_c$ (Luna & McConnell, 1977). As the temperature is raised above the main transition, the lipid adopts a one-dimensional lamellar $L_\alpha$ phase with the acyl chains disordered and, on the average, parallel to the bilayer normal. On the basis of these observations and a variety of thermodynamic and spectroscopic investigations, the main transition is described as an order–disorder or melting transition of the acyl chains.

Aside from the appearance of the two-dimensional rippled lattice, no molecular description of the pretransition is apparent. Unpublished $^2H$ NMR results from this laboratory on DMPC samples specifically deuterated in the acyl chains show no precipitous changes in the residual quadrupolar coupling constants in the neighborhood of the pretransition. Similar negative results have been reported for phosphatidylcholines specifically deuterated in the choline head group and from $^{31}P$ NMR studies of the residual chemical shift anisotropy (R. J. Wittebort and R. G. Griffin, unpublished results; Gally et al., 1975). Herein we report on $^{13}C$ NMR studies of dipalmitoylphosphatidylcholine specifically labeled with $^{13}C$ at the carbonyl position of the 2 chain, 2-[1-$^{13}$C]-DPPC. We find that at temperature values in the neighborhood of $T_c'$, the $^{13}C$ NMR spectra indicate the presence of two or more motionally or conformationally inequivalent populations of carbonyl atoms.

## Experimental Procedures

Samples of 2-[1-$^{13}$C]DPPC were prepared by acylation of lysopalmitoyl-PC with [1-$^{13}$C]palmitic acid by using the procedure of Boss et al. (1975). Purification was accomplished by chromatography on silica gel. For the NMR experiments, ~50 mg of lipid was placed in a tube with a constriction, an equal weight of $H_2O$ was added with a syringe, and the sample was sealed under high vacuum. $^{13}C$ NMR spectra were obtained on a home-built spectrometer operating at 6.8 T (74 MHz for $^{13}C$, 294 MHz for $^1H$). Spectra of the dry powders were obtained by using standard cross-polarization together with a 180° refocusing pulse at the $^{13}C$ frequency to circumvent receiver overload (Pines et al., 1973). For the lipid–$H_2O$ samples, the $^{13}C$ $T_1$ was sufficiently short that cross-polarization was unnecessary. Thus, a simple Hahn spin echo was employed to collect the spectra of the dispersed lipid. A typical $\pi/2$ $^{13}C$ pulse was 4 μs. With strong $^1H$ decoupling fields, it is quite easy to produce significant sample heating (≳10 °C). Since the spectral changes described here are strongly temperature dependent, they could be produced by radio-frequency (rf) heating alone; consequently, we have been particularly careful to ensure that this was not the case. For example, we have used the minimum decoupling power necessary to obtain sharp spectra and have examined undecoupled spectra as well. This point is discussed further below. Temperature control was achieved with a gas flow system where the gas was blown directly onto the rf sample coil. Since the coil consisted of approximately seven turns of heavy copper wire with the sample in the center, it is a good approximation to a constant temperature oven, and we have not been able to measure thermal gradients in the sample. Moreover, since the gradients would have to be ~15 °C (which is at least an order of magnitude larger than we believe them to be), we can exclude this as a possible source of the observed spectral effects.

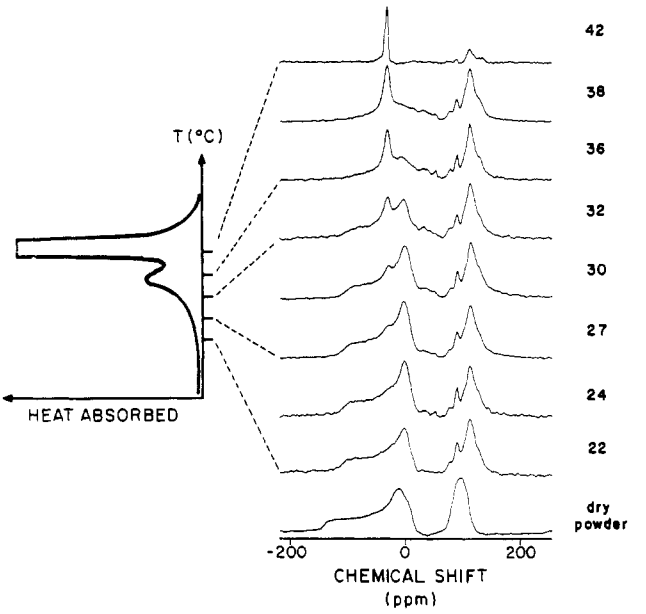


FIGURE 1: Proton-decoupled 74-MHz $^{13}C$ spectra of 2-[1-$^{13}$C]DPPC. The bottom spectrum in the figure was obtained from a dry powder by using cross-polarization techniques. The remaining spectra were obtained with a Hahn echo from a 50 wt % $H_2O$ sample as a function of temperature (°C). Chemical shifts are relative to external $C_6H_6$. Shown also is a calorimetric trace obtained following the NMR experiments. The dashed lines show the position of the NMR spectra relative to the temperatures of the calorimetric pre- and main transitions.

Calorimetric measurements were kindly performed by Dr. G. G. Shipley of Boston University on a Perkin-Elmer DSC-2. The DSC trace shown in Figure 1 was obtained at a scan rate of 5 °C/min, and the sample consisted of 29 mg of the 50 wt % $H_2O$ NMR sample. While the trace shown in Figure 1 does not represent the ultimate resolution obtainable in a DSC experiment, it does confirm the presence of a pretransition in the particular sample on which the NMR experiments were performed.

## Results

Shown in Figure 1 are $^{13}C$ NMR spectra of 2-[1-$^{13}$C]DPPC. The lower trace was obtained from the dry powder whereas the upper traces were obtained as a function of temperature from aqueous dispersions containing 50 wt % $H_2O$. After completion of the NMR experiment, the sample was examined calorimetrically to ensure that the lipid did indeed exhibit a pretransition. Thus, the DSC trace clearly showing the pretransition and the NMR spectra of Figure 1 were obtained from the same sample. The envelope of resonances extending from 65 to 146 ppm arises from the protonated carbons of the acyl chains, glycerol backbone, and choline head group. In the spectral region between −140 and 25 ppm, the dry lipid gives a characteristic $^{13}C$ carbonyl powder pattern arising from the single $^{13}C$-enriched site. The slightly asymmetric pattern has a total breadth, $\Delta\sigma \equiv \sigma_{11} - \sigma_{33}$, of −148 ppm and principal components of $\sigma_{11} = -134$ ppm, $\sigma_{22} = -8$ ppm, and $\sigma_{33} = 14$ ppm relative to external $C_6H_6$. At temperature values between 0 and 24 °C, the dispersed lipid shows an axially symmetric pattern with a residual anisotropy, $\langle\Delta\sigma\rangle = \sigma_{\parallel} - \sigma_{\perp}$, of −112 ppm, while at lower temperatures ($T \leq -20$ °C), this pattern

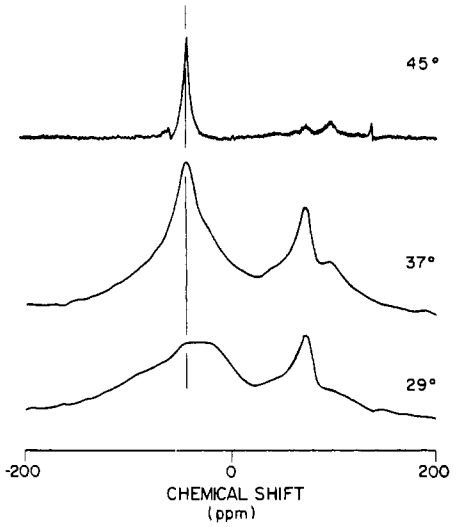


FIGURE 2: Proton-coupled spectra of 2-[1-$^{13}$C]DPPC as a function of temperature in the $L_{\beta'}$ (bottom), $P_{\beta'}$ (middle), and $L_\alpha$ (top) phases. These spectra exhibit the features observed in the decoupled spectra of Figure 1, and they indicate that the spectral patterns are not artifacts arising from rf heating of the sample. Chemical shifts are relative to external $C_6H_6$.

converts to the axially asymmetric dry powder spectrum. The reduced breadth of the well-delineated spectrum observed for temperatures between 0 and 24 °C indicates that the lipid molecules in the dispersed sample undergo some type of anisotropic motion that is fast compared to $\gamma H_0 \Delta\sigma \approx 10^4$ s$^{-1}$.

As the temperature is raised to the onset of the thermal pretransition, 27 °C, the observed pattern shows the presence of at least two overlapping spectral components. The predominant contribution is an $L_{\beta'}$-like axially symmetric pattern with $\langle\Delta\sigma\rangle = -112$ ppm whereas the less dominant pattern is a symmetric line of width ~1 kHz. The chemical shift of this line, $\langle\sigma\rangle = -44$ ppm, is that expected if the tensor values determined for the dry lipid are completely averaged, i.e., $\langle\sigma\rangle = {}^1/_3(\sigma_{11} + \sigma_{22} + \sigma_{33})$. From Figure 1, we see that with further increases in temperature the narrow component increases in intensity, and for $T > T_c = 42$ °C, only this component is observed, with an effective line width (including a substantial instrumental contribution) of 500 Hz.

In these experiments, moderate power $^1$H decoupling (50 W) is applied during the dephasing, refocusing, and acquisition periods of the Hahn echo sequence. Consequently, an artifactual reason for the appearance of the $L_\alpha$-like pattern ($|\langle\Delta\sigma\rangle| \lesssim 7$ ppm) at temperatures below $T_c$ would be the presence of a large thermal gradient in the sample arising from rf heating. Shown in Figure 2 are spectra obtained without $^1$H decoupling at 45 ($L_\alpha$ phase), 37 ($P_{\beta'}$ phase), and 29 °C ($L_{\beta'}$ phase). The features observed in the spectra obtained with $^1$H decoupling (Figure 1) are broadened by residual $^{13}$C–$^1$H dipolar couplings. However, the characteristic spectral features due to chemical shift anisotropy remain. In particular, the sharp $L_\alpha$-like peak seen clearly in the 45 °C spectrum (Figure 2) is also clearly visible in the 37 °C $P_{\beta'}$ phase spectrum and, as expected, nearly absent in the 29 °C spectrum.

Shown in Figure 3 are transverse relaxation, i.e., spin echo, experiments obtained from this sample in the $L_\alpha$, $P_{\beta'}$ and $L_{\beta'}$ phases. The indicated $\tau$ values are the delay times in the Hahn echo experiment. Immediately apparent is the large increase in the transverse relaxation rate in the intermediate $P_{\beta'}$ phase ($T_2 = 0.30$ ms) relative to either the high temperature $L_\alpha$ ($T_2 = 7.2$ ms) or low temperature $L_{\beta'}$ ($T_2 = 1.6$ ms) phases.

## Discussion

In Figure 4 the effect on a $^{13}$C powder pattern of axial molecular motion of varying rate is shown in several spectral simulations. The line shapes, which were computed with methods described previously (Campbell et al., 1979), are determined by two parameters, the correlation time of the motion, $\tau_c$, and the angle $\theta$ between the unique shielding tensor axis and the axis of motion. For these simulations, $\theta = 54°$ 44′, i.e., the magic angle, and we vary the reduced rate parameter $\Omega \equiv (\tau\Delta\sigma\gamma H_0)^{-1}$ from the slow motion limit ($\Omega < 0.1$) to the fast motion limit ($\Omega > 10$). In the slow range ($\Omega \lesssim 0.05$), the characteristic powder pattern which is independent of $\theta$ and $\tau_c$ is obtained. In the fast exchange limit ($\Omega \gtrsim 10$),

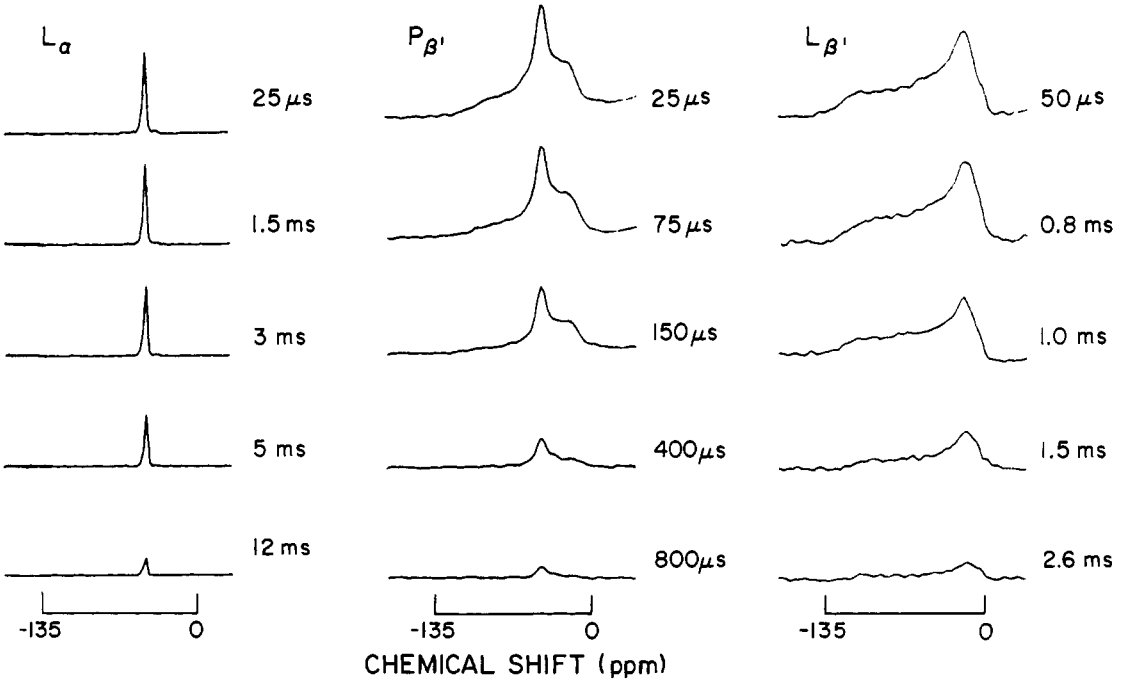


FIGURE 3: Representative transverse relaxation spectra obtained with a Hahn echo. The number beside each spectrum is the $\tau$ value. Note the substantially shorter $T_2$ exhibited by the $P_{\beta'}$ phase ($T_2 = 0.3$ ms and $T = 37$ °C) as opposed to the $L_{\beta'}$ phase ($T_2 = 1.6$ ms and $T = 20$ °C) and the $L_\alpha$ phase ($T_2 = 7.2$ ms and $T = 48$ °C). The chemical shift scale is arbitrary.

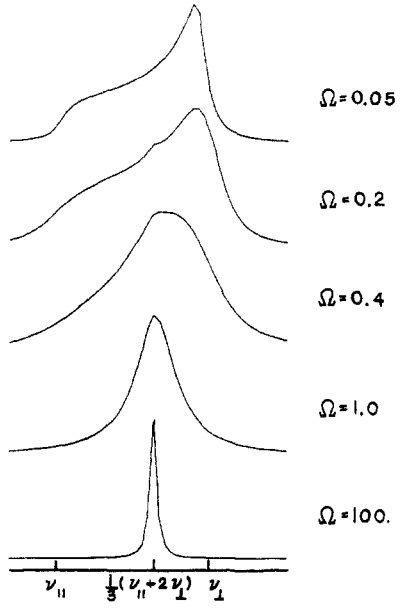


FIGURE 4: Spectral simulations showing the effect of axial motion of various rates on an axially symmetric shielding tensor. The unique axis of the axially symmetric tensor was assumed to be oriented at the magic angle with respect to the diffusion axis, and the reduced diffusion parameter $\Omega = [\tau\Delta\sigma\gamma H_0]^{-1}$ used in each simulation is shown in the figure.

a collapsed pattern with well-delineated features is obtained but reduced in breadth by a factor of $^1/_2(3\cos^2\theta - 1)$ which is zero for the chosen value of $\theta$. In contrast, in the intermediate range ($0.2 < \Omega < 10$), the spectral line shapes lack well-resolved features which, unlike the fast limit spectrum, depend on $\tau_c$ as well as $\theta$. With the possible exception of those obtained at 36 and 38 °C, the experimental spectra in Figure 1 (and those in Figure 3 at short $\tau$ values) show both well-resolved features and a reduced breadth compared to the dry powder spectrum. Thus, these experimental results demonstrate the presence of rapid motion. Consequently, the shapes, i.e., the residual anisotropies of these patterns, are determined essentially by the orientation of the $^{13}C$ shielding tensor relative to the axis of motion. For convenience, then, we can consider the temperature dependence of the spectra in Figure 1 as arising from a conformational change shifting the orientation of the $^{13}C$ carbonyl shielding tensor relative to the axes of motion and/or a large change in the rate (from $\Omega < 0.1$ to $\Omega > 10$ or vice versa) and amplitude of thermal motion(s) executed by the lipid molecule at the site of the single $^{13}C$ label. We now consider the experimental spectra in the context of these two types of alterations.

There are three trivial explanations of the spectra in Figure 1, and these are that the narrow component is due to the appearance of an isotropically tumbling lipid fraction, to the presence of an impurity, or to the coexistence of two or more phases. All three possibilities can be excluded for the following reasons. If an isotropically tumbling fraction were present, then anomalously narrow lines would appear in the glycerol acyl chain region of the spectrum, and these are clearly not present. In addition, a sharp component would appear in $^{31}P$ spectra, and again this is not observed. It is known that impurities such as fatty acids can alter the phase behavior of lipid bilayers, and thus their presence might also induce the appearance of the narrow in the $^{13}C$ spectra. However, TLC's taken after completion of the experiment showed only pure lipid. In addition, if impurities are present, then the pretransition is usually not observed (G. G. Shipley, private communication). The calorimetric trace in Figure 1 does show a pretransition, and this is further evidence that the observed spectral effects are not due to the presence of impurities. Finally, it is possible that the spectra of Figure 1 could be due to the simultaneous presence of two phases. Indeed, in mixtures of DPPC and DPPE at temperatures and compositions where it is expected to have two phases simultaneously present, spectra consisting of a superposition of sharp and narrow components such as those shown in Figure 1 are observed (A. Blume, D. M. Rice, and R. G. Griffin, unpublished results). However, at present there is no evidence for the existence of more than a single phase for pure lecithin bilayers in the pretransition region.

It is useful to note that the 2-chain carbonyl group is in a nearly "rigid" part of the molecule insensitive to acyl chain or choline head-group motions. Thus, at least for temperatures above $T_c$, an important factor in determining the $^{13}C$ spectral line shape is the axial diffusive motion of the lipid molecule about its long axis. If we assume that, at temperatures below as well as above $T_c$, this axial motion predominates and is fast ($1/\tau_c > 10^4\ s^{-1}$), then the change in the residual anisotropies, $\langle\Delta\sigma\rangle$, could be explained solely by invoking a conformational change which shifts the orientation of the shielding tensor relative to the long axis of the molecule. If we make the good approximation that the shift tensor has axial symmetry, then the residual anisotropy is given by $\langle\Delta\sigma\rangle = \Delta\sigma \times {}^1/_2(3\cos^2\theta - 1)$ where $\theta$ is the angle between the unique shielding tensor axis, $\sigma_{11}$, and the long axis of the lipid molecule and $\Delta\sigma$ is the rigid lattice tensor breadth. For $|\langle\Delta\sigma\rangle| \lesssim 7$ ppm ($T > T_c$), $\theta = 54°$, and for $|\langle\Delta\sigma\rangle| = 112$ ppm ($T < T_c'$), $\theta = 24°$.

The X-ray structure of DMPC dihydrate recrystallized from ether/ethanol/water solution shows two molecules per unit cell with different structures (Pearson & Pascher, 1979). In these two structures, the *sn*-2 carbonyl bond makes an angle of 80° and 61° with respect to the chain axis (R. H. Pearson, private communication). To compare directly the X-ray structure with the results in this work requires a knowledge of the molecular orientation of the ester $^{13}C$ shielding tensor. On the basis of limited tensor data from model compounds, we assume that the unique tensor component, $\sigma_{11}$, is along the C=O bond and the $\sigma_{33}$ element is approximately perpendicular to the ester group plane (Pines & Abramson 1974). The calculated difference in the tensor orientation of 30° can then be directly compared with the 19° difference in the *sn*-2 carbonyl bond directions in the two molecular conformations in crystalline DMPC. This apparent discrepancy is subject to further refinement of both the crystallographic angles, which have an uncertainty of ±5° at present, as well as the molecular orientation of the shielding tensor. We should note that if the two patterns of $|\langle\Delta\sigma\rangle| = 112$ ppm and $|\langle\Delta\sigma\rangle| \lesssim 7$ ppm are associated with the two crystallographic structures, then the spectra of Figure 1 require that only in the intermediate $P_{\beta'}$ phase, and not the $L_\alpha$ or low temperature $L_{\beta'}$ phases, do the two structures coexist.

In connection with this point, we should mention that the suggestion in the literature of the presence of two long-lived conformations in the glycerol backbone region of lecithins in the $L_\alpha$ phase appears to be incorrect. In particular, two $^2H$ NMR signals are observed from $^2H$'s at the 2 position of the *sn*-2 chain (Seelig & Seelig, 1975), and a similar phenomenon occurs at the 3 position of the glycerol moiety when it is racemically labeled (Gally et al., 1975). Initially it was suggested that these pairs of signals might be due to the simultaneous presence of two different long-lived molecular conformations in the phase. However, recent studies of compounds with optically active labels show only a single line in

each case, and thus the two signals must arise from two magnetically inequivalent $^2$H's (A. Engel and D. Cowburn, private communication; J. Seelig, private communication). Moreover, spectra of DMPC labeled at the 2 position of the glycerol show a single splitting (R. J. Wittebort, V. Rios-Mercadillo, R. G. Griffin, and G. M. Whitesides, unpublished results), and in the $^{13}$C spectra presented here, a single line is observed in the $L_\alpha$ phase. Collectively these observations suggest that in the $L_\alpha$ phase the glycerol region of the molecule either assumes a single, reasonably rigid conformation or that there is fast rather than slow exchange among conformations. This point will be discussed in more detail in a future publication (R. J. Wittebort, V. Rios-Mercadillo, R. G. Griffin, and G. M. Whitesides, unpublished results). Nevertheless, the conformational changes which we discuss here are associated with transitions between the $L_{\beta'}$ and $P_{\beta'}$ and the $P_{\beta'}$ and $L_\alpha$ phases and should be clearly distinguished from those proposed for the $L_\alpha$ phase alone.

A formally equivalent interpretation of the $\theta$ values calculated above is that the change in residual anisotropy results from a $\sim$30° shift in the orientation of the diffusion axis relative to the long molecular axis. Since X-ray experiments indicate a chain tilt of $\sim$30° in the $L_{\beta'}$ phase and 0° in the $L_\alpha$ phase and thus $\Delta\theta = 30°$, this explanation merits consideration. In both the $L_{\beta'}$ and $L_\alpha$ phases, the observed patterns are sharp; consequently we would require that the motion about the diffusion axis be fast. This interpretation requires that in the $L_{\beta'}$ phase there is a precession-like motion of the lipid molecules on the surface of a cone where the long axis of the molecule subtends an angle of 30° with respect to the diffusion axis. As the temperature approaches $T_c'$, a fraction of the molecules begin to align themselves along the diffusion axis, and, finally above $T_c$, where the narrow line is observed, they all would have their long axes coincident with the diffusion axis. The axis of motion is, however, expected to be coincident with the long molecular axis at all temperatures, and thus we currently do not favor this explanation.

Now we consider the alternative possibility that the orientation of the carbonyl tensor is at the "magic angle" with respect to the diffusion axis in the $L_{\beta'}$, $P_{\beta'}$, and $L_\alpha$ phases, but the overall motion of the lipid molecule in the $L_{\beta'}$ phase is different in terms of rate and amplitude from that in the $L_\alpha$ phase. Again, since the characteristic $L_{\beta'}$ phase spectrum is sharp, the correlation time for any motion present must, roughly speaking, be either long or short compared to $\gamma H_0 \Delta\sigma$. In particular, we now assume that the axial motion is effectively frozen out on this time scale. Thus a powder pattern approaching the rigid lattice breadth of 142 ppm and exhibiting some asymmetry is expected. Since an axially symmetric spectrum with $|\langle\Delta\sigma\rangle| = 112$ ppm is observed in the $L_{\beta'}$ phase, it must be assumed that there are other motions present, presumably small amplitude librational modes which result in this observed spectrum.

Within this model the observed spectra of Figure 1 arise in the following manner. As the temperature is increased to the onset of the pretransition, some of the molecules in the bilayer begin to execute rapid axial motion. Because the shift tensor is oriented at the magic angle ($\theta = 54°$), these rotating molecules give rise to a $\langle\Delta\sigma\rangle \approx 0$ component. As the temperature is raised further, this component, satisfying the dynamical constraint that $\tau_c^{-1} > \gamma H_0 \Delta\sigma$, grows at the expense of the $\langle\Delta\sigma\rangle = 112$ ppm component. For $T > T_c$, all molecules diffuse rapidly, and only the narrow line remains. The rippled structure of the $P_{\beta'}$ lattice, as described by Janiak et al. (1976), could apparently accommodate this dynamical inequivalence. Proceeding along the ripple profile, not all molecules are equivalently oriented relative to the local bilayer normal, and their axial motion could be more or less quenched by the local periodic packing. Thus the pretransition and the formation of the ripple phase could be associated with the appearance of a fraction of molecules in the bilayer which appear liquid-crystalline-like simply because of their increased axial diffusion rates.

There are a number of experimental results, in addition to those presented here, which could be interpreted as supporting this hypothesis. In particular, X-ray ESR, and other NMR experiments have detected changes in the appropriate physical parameters which suggest the presence of liquid-crystalline-like molecules and increased axial diffusion rates in the neighborhood of the pretransition. X-ray studies have shown that the lattice changes from a distorted to a regular hexagonal arrangement at the pretransition (Janiak et al., 1976) such as is found above $T_c$, and this could accommodate increased axial diffusion rates. In ESR Tempo (2,2,6,6-tetramethylpiperidinyl-1-oxy) solubility experiments, the Tempo spectral parameter is observed to increase at the pretransition, indicating the appearance of liquid-crystalline-like molecules (Luna & McConnell, 1977). Moreover, recent saturation transfer ESR measurements suggest the presence of two correlation times for axial diffusion of $\sim 10^{-4}$ and $\sim 10^{-6}$ s at temperatures near the pretransition (Marsh, 1980). An analysis of the temperature dependence of the $^{31}$P NMR line shapes has also suggested that conformation changes occur at the head group and axial diffusion rates increase at the pretransition. In particular, the perpendicular edge of the axially symmetric $^{31}$P powder spectrum increases in intensity relative to the parallel edge in going from 25 to 35 °C, and it was necessary to raise the diffusion rates and readjust the rigid lattice tensor orientation in order to successfully simulate these spectra (Campbell et al., 1979). Finally, $^2$H NMR experiments on specifically labeled lecithins performed in this laboratory also could be interpreted as supporting this hypothesis. For example, spectra of [$^2$H]glycerol-labeled lecithins clearly show the presence of two or more components, and the narrower of the two grows at the expense of the broad component with increasing temperature. In summary, there is ample evidence that axial diffusion rates increase at the pretransition, and it is possible that this effect alone could explain the appearance of the $\langle\Delta\sigma\rangle \approx 0$ component in the $^{13}$C=O spectra.

While we believe that increased axial diffusion rates may contribute to the observed spectral narrowing, there are several features of the experimental data which suggest that this alone is not sufficient to explain the results. First, with this model, the $L_{\beta'}$ structure is assumed to be quite rigid, the only motions affecting the $^{13}$C label being the postulated librational modes. Such modes are very inefficient in effecting nuclear magnetic relaxation (Wittebort & Szabo, 1978). Moreover, in rigid systems it is generally necessary to employ cross-polarization to obtain the spectrum. For example, to obtain $^{13}$C=O spectra of glycolipids, which do not rotate in their crystalline phase below $T_c$, this is the case (Huang et al., 1980), and it is also true for dry powders or frozen aqueous dispersions of lecithins and phosphatidylethanolamines. However, in the hydrated lecithin samples, a Hahn echo with a recycle delay of 5 s is sufficient to obtain an unsaturated spectrum (i.e., $T_1 \lesssim 2$ s). Also, the observed residual $L_{\beta'}$ pattern has axial symmetry, and a motional process consistent with this must be assumed. Librational motions typically yield an averaged pattern with nonaxial character. Finally, the simulations the Figure 4 show

that with the unique axis of the tensor tilted at the magic angle, the result of increasing the axial diffusion rate is a line shape with *broadened* perpendicular and parallel edges which gradually collapses to an isotropic-like line. Thus, the relative short $T_1$ and the observation of the *sharp* axially symmetric line shape suggest that the $|\langle\Delta\sigma\rangle| = 112$ ppm $L_{\beta'}$ pattern is not due to the absence or near absence of axial motion. Additionally we note that a more accurate condition for fast motion depends on the difference of the breadths of the static and averaged patterns. To reduce the static pattern ($\Delta\sigma$ = 142 ppm) to the $L_\alpha$-like pattern requires $1/\tau_c > 10^4$ $s^{-1}$ whereas to reduce it to the $L_{\beta'}$-like pattern requires only $1/\tau_c > 10^3$ $s^{-1}$, a rather slow molecular motion.

In summary, we propose the following features for the lecithin $L_{\beta'} \rightarrow P_{\beta'}$ and $P_{\beta'} \rightarrow L_\alpha$ phase transitions which provide a consistent interpretation of the reported $^{13}C$ spectral data. In the $L_{\beta'}$ phase, the unique axis of the *sn*-2 chain $^{13}C$ ester shielding tensor, $\sigma_{11}$, makes an angle of $\sim 24°$ with respect to the long axis of the lipid molecule, and the motion about this axis is sufficiently rapid to produce a fast limit, axially symmetric spectrum. For production of this spectrum, $1/\tau_c > 10^3$ $s^{-1}$ is required, although a shorter correlation time is not excluded by our results. As the temperature is raised to the onset of the pretransition ($T \approx 30$ °C for DPPC), some of the lecithin molecules begin to adopt features of the $L_\alpha$ phase. In particular, the $\langle\Delta\sigma\rangle \simeq 0$ component appears and increases in intensity as the temperature is further increased. As mentioned above, there is abundant evidence of increased axial diffusion rates in the $P_{\beta'}$ phase, and these may contribute to the narrowing of the $\langle\Delta\sigma\rangle \simeq 0$ component. However, even at 37 °C, the residual $L_{\beta'}$-like pattern remains sharp, as is shown in the top ($\tau$ = 25 $\mu$s) spectrum of Figure 3, and this suggests that two long-lived conformations coexist in this phase. Thus, we associate with the pretransition a conformational transition shifting the orientation of unique axis of the shielding tensor by 30°. It is possible that the two postulated conformations could be associated with the two conformations observed in crystallographic studies (Pearson & Pascher, 1979). The relaxation data of Figure 3 suggest that there may be exchange between these conformations. The $T_2$ values are comparatively long in the $L_{\beta'}$ and $L_\alpha$ phases (1.6 and 7.2 ms, respectively) where only single conformations exist, but become short ($T_2$ = 0.30 ms) in the $P_{\beta'}$ phase due to exchange broadening between the two (or more) conformations. For $T > T_c$, the conformational transition is complete, the axial diffusion rates are fast, and a single narrow line is observed in the $L_\alpha$ phase.

Finally we should mention one additional experimental observation which supports this interpretation. The $^2H$ spectra of acyl chain labeled DPPE's exhibit spectra which are interpretable as an all-trans chain undergoing fast axial diffusion for temperatures about 10 °C below $T_c$, e.g., $1/\tau_c > 10^5$ s. Thus, for these temperatures, the axial motion is most certainly fast on the $^{13}C$ time scale. At the same temperatures, $^{13}C$ spectra of *sn*-2 C=O labeled DPPE yield an axially symmetric powder spectrum identical with that observed for the $L_{\beta'}$ phase of DPPC. Finally, for $T > T_c = 63$ °C, the $^{13}C$ powder pattern collapses to a $\langle\Delta\sigma\rangle \simeq 0$ component as observed with DPPC (A. Blume, D. M. Rice, R. J. Wittebort, and R. G. Griffin, unpublished results). Since the motion is fast on the $^{13}C$ time scale for temperatures below and above $T_c$, the observed spectra collapse must be due to a conformational change such as has been postulated here for DPPC.

## Conclusions

$^{13}C$ NMR spectra 2-[1-$^{13}C$]DPPC exhibit a remarkable temperature dependence. At low temperatures when the lipid is in the $L_{\beta'}$ phase, an axially symmetric powder spectrum with $|\langle\Delta\sigma\rangle| = 112$ ppm breadth is observed, and this spectrum transforms to an isotropic-like line in the $L_\alpha$ phase with $\langle\Delta\sigma\rangle \leq 7$ ppm. At intermediate temperatures corresponding to the monoclinic $P_{\beta'}$ phase, a superposition of the spectral patterns is observed. Several explanations of the temperature dependence are possible, but it appears that the most plausible explanation must involve a conformational change at the *sn*-2 carbonyl. The results reported here, along with other results cited above, illustrate that an important feature of the monoclinic phase of hydrated lecithins is the coexistence of gel and liquid-crystalline-like molecules in the bilayer. Associated with the liquid-crystalline-like fraction are increased rates of axial diffusion as well as the postulated conformation change. Thus, the $P_{\beta'}$ phase is not one with its own unique set of structural and/or dynamical properties; rather, it exhibits characteristics of both the $L_{\beta'}$ and $L_\alpha$ phases, and therefore any microscopic model of this phase should be consistent with these observations.

## Acknowledgments

Thanks are accorded to G. G. Shipley for performing calorimetric measurements and to A. McLaughlin for conversations during the early stages of this work.

## References

Boss, W. F., Kelly, C. F., & Landsberger, F. R. (1975) *Anal. Biochem. 64*, 289–292.

Campbell, R. F., Meriovitch, E., & Freed, J. H. (1979) *J. Phys. Chem. 83*, 525–533.

Chapman, D., Williams, R. M., & Ladbrooke, B. D. (1967) *Chem. Phys. Lipids 1*, 445–475.

Gally, U., Niederberger, W., & Seelig, J. (1975) *Biochemistry 14*, 3647–3652.

Huang, T. H., Skarjune, R., Wittebort, R. J., Griffin, R. G., & Oldfield, E. (1980) *J. Am. Chem. Soc. 102*, 7377–7379.

Janiak, M. J., Small, D. M., & Shipley, G. G. (1976) *Biochemistry 15*, 4575–4586.

Janiak, M. J., Small, D. M., & Shipley, G. G. (1979) *J. Biol. Chem. 254*, 6068–6078.

Luna, E. J., & McConnell, H. M. (1977) *Biochim. Biophys. Acta 466*, 381–392.

Marsh, D. (1980) *Biochemistry 19*, 1632–1637.

Pearson, R. H., & Pascher, I. (1979) *Nature (London) 281*, 499–501.

Pines, A., & Abramson, E. (1974) *J. Chem. Phys. 60*, 5130–5131.

Pines, A., Gibby, M. G., & Waugh, J. S. (1973) *J. Chem. Phys. 59*, 569–590.

Seelig, A., & Seelig, J. (1975) *Biochim. Biophys. Acta 406*, 1–5.

Stamatoff, J. B., Graddick, W. F., Powers, L. F., & Moncton, D. E. (1979) *Biophys. J. 25*, 253–262.

Tardieu, A., Luzatti, V., & Reman, F. C. (1973) *J. Mol. Biol. 75*, 711–733.

Wittebort, R. J., & Szabo, A. (1978) *J. Chem. Phys. 69*, 1722–1736.